J Biomol NMR (2008) 40:145–152
DOI 10.1007/s10858-007-9217-z

ARTICLE

Tuning the HNN experiment: generation of serine–threonine check points

Jeetender Chugh · Dinesh Kumar · Ramakrishna V. Hosur

Received: 8 November 2007 / Accepted: 13 December 2007 / Published online: 28 December 2007

Abstract We describe here the tunability of the HNN experiment to obtain certain residue specific peak patterns in the spectra of (^{15}N, ^{13}C) labeled proteins. This is achieved by tuning a band-selective 180° pulse on the carbon channel in the pulse sequence, whereby one can tamper with the C^{α}–C^{β} coupling evolutions for the different residues. Specifically, we generate distinctive peak patterns for serine and threonine and their neighbors in the different planes of the three dimensional spectrum. These provide useful anchor points during sequential assignment of backbone resonances. The performance of this experiment, referred to as HNN-ST here, is demonstrated using two proteins, one properly folded and the other completely denatured. With the availability of high field spectrometers, techniques such as TROSY, and ever increasing sensitivities in the probes, this experiment with its large number of check points has a great potential for rapid and unambiguous backbone resonance assignment in large proteins.

Keywords Band-selective pulse · Check points · HNN · HNN-ST · NMR

Introduction

The development of multi-dimensional triple resonance NMR experiments has helped a great deal in the structure elucidation of proteins in aqueous solutions. In this context, we had earlier described two triple-resonance NMR experiments, HNN and HN(C)N (Panchal et al. 2001). These experiments, derived by modification of HN(CA)NNH (Weisemann et al. 1993) and HN(COCA)NH (Bracken et al. 1997; Grzesiek et al. 1993; Matsuo et al. 1996) described previously, enabled rapid assignment (Bhavesh et al. 2001; Chatterjee et al. 2002) of H^N and ^{15}N atoms of amino acid residues in folded as well as unfolded proteins. The magnetization transfer pathways employed in these experiments have been recently used along with projection principles to generate six and seven dimensional experiments called as APSY-6d and APSY-7d, respectively (Fiorito et al. 2006; Hiller et al. 2007).

The main strength of the HNN and the HN(C)N experiments, as against the standard triple resonance experiments currently being used for backbone assignments [reviewed in Permi and Annila (2003)], or even the recent APSY experiments, lies in the fact that the various planes in the 3D spectra of HNN and HN(C)N contain positive and negative peaks, and the patterns of their combinations in any plane reflect upon the particular types of triplet sequences of amino acid residues along the polypeptide chain (Bhavesh et al. 2001; Chatterjee et al. 2002). Special patterns arise around glycines and prolines and they serve as start/check points during a sequential resonance assignment walk. The generally good dispersion of ^{15}N chemical shifts in both folded and unfolded/denatured proteins does not pose cancellation of positive and negative intensities as a serious bottleneck and the sequential walks can be completed in most cases. This advantage of peak patterns HNN and HN(C)N is in addition to the fact that they provide direct correlations in the ^{15}N plane of a particular residue to its neighboring residues, which is also provided by the HN(CA)NNH

J. Chugh · D. Kumar · R. V. Hosur (✉)
Department of Chemical Sciences, Tata Institute of Fundamental Research, 1, Homi Bhabha Road, Colaba, Mumbai 400005, India
e-mail: hosur@tifr.res.in

(Weisemann et al. 1993) and HN(COCA)NH (Bracken et al. 1997; Grzesiek et al. 1993; Matsuo et al. 1996) experiments.

In this paper, we demonstrate further the unrecognized versatility and potential of the HNN experiment. We show that the experiment can be tuned differently to put emphasis on other kinds of triplet stretches. The HNN-A experiment (Chatterjee et al. 2006) recently described turned out to be one particular application where the alanines were highlighted. Here we show how HNN can be tuned to emphasize serines and threonines in the 3D spectra. This particular experiment will be termed hereafter as HNN-ST. The specific modification described here generates many more check points which would significantly enhance the speed and correctness of backbone assignments. The performance of the experiment has been demonstrated with two protein systems, one folded [M-Crystallin (apo form), an important Ca^{2+}-binding protein of the $\beta\gamma$-crystallin superfamily from the *Methanosarcina acetivorans*] and the other denatured (8 M urea-denatured dsmt3, the SUMO protein from *Drosophila melanogaster*).

Materials and methods

Protein expression and purification

^{15}N–^{13}C labeled dsmt3 protein was expressed and purified as described elsewhere (Kumar et al. 2007). ^{15}N–^{13}C labeled apo M-crystallin (Barnwal et al. 2006) was obtained as a kind gift from Ravi P. Barnwal.

NMR spectroscopy

All NMR experiments were performed at 25°C on a Bruker Avance spectrometer equipped with a CryoProbe, operating at ^{1}H frequency of 800 MHz. For both HNN and HNN-ST experiments, the delays $2T_N$ and 2τ were set to 30 and 25 ms, respectively. Forty complex points were used along $F_1(^{15}N)$ and $F_2(^{15}N)$ dimensions in case of urea-denatured dsmt3 and 32 points in case of folded M-crystallin protein. In $F_3(H^N)$ dimension, 1,024 complex points were collected for both the proteins. Sixteen scans were recorded for each FID. The acquisition time for each of the experiments was approximately 36 h for unfolded protein (urea-denatured dsmt3) and 22 h for folded protein (apo M-crystallin), respectively. For the HNN-ST experiment, a band selective $C^{\alpha/\beta}$ inversion pulse was applied using a standard Gaussian cascade Q3 pulse (Emsley and Bodenhausen 1990). The pulse width used was 600 μs (at 13.98 W) and the bandwidth was ~6,000 Hz. The carbon carrier frequency was placed at 56 ppm and the carrier for the selective pulse (encircled pulse, Fig. 1) on carbon channel was placed at 64 ppm.

Results and discussion

Tuning and versatility of HNN

The HNN experiment (Fig. 1) uses the following magnetization transfer pathway (Panchal et al. 2001):

$$\mathrm{H}_i^N \rightarrow \mathrm{N}_i(t_1) \xrightarrow{2T_N} \mathrm{C}^{\alpha}_{i-1,i} \xrightarrow{2\tau} \mathrm{N}_{i-1,i,i+1}(t_2) \rightarrow \mathrm{H}_{i-1,i,i+1}(t_3) \quad (1)$$

The pulse sequence in Fig. 1 differs slightly from the original sequence in that it uses the WATERGATE (Piotto et al. 1992) sequence before detection for better water suppression and as a consequence the 'sensitivity enhancement' part has been dropped; frequency selection along the two indirect dimensions was done by States-TPPI method (Marion et al. 1989). In the 3D spectrum the peaks appear at the coordinates:

$$F_1 = \mathrm{N}_i, (F_3, F_2) = (\mathrm{H}_i, \mathrm{N}_i),\ (\mathrm{H}_{i-1},\ \mathrm{N}_{i-1}),\ (\mathrm{H}_{i+1},\ \mathrm{N}_{i+1})$$
$$F_2 = \mathrm{N}_i,\ (F_3, F_1) = (\mathrm{H}_i, \mathrm{N}_i),\ (\mathrm{H}_i,\ \mathrm{N}_{i-1}),\ (\mathrm{H}_i,\ \mathrm{N}_{i+1})$$

Thus, in each plane there occurs a diagonal peak ($F_1 = F_2 = \mathrm{N}_i$) for each residue and there are two sequential peaks to residues ($i - 1$) and ($i + 1$). In a chain of four residues, $i - 2$ to $i + 1$, the intensities of the diagonal $\left(I_i^d\right)$ and cross $\left(I_{i-1}^c, I_{i+1}^c\right)$ peaks in the (F_2, F_3) planes of the HNN spectrum are given by (Chatterjee et al. 2006):

$$I_i^d = -\left(E_1^2 E_3 E_9 K_{i1}^d + E_2^2 E_5 E_{10} K_{i2}^d\right) \quad (2)$$

$$I_{i-1}^c = E_1 E_4 E_7 E_9 K_{i-1}^c; \quad I_{i+1}^c = E_2 E_6 E_8 E_{10} K_{i+1}^c \quad (3)$$

where,

$$\begin{aligned} E_1 &= \cos p_i T_N \sin q_{i-1} T_N \\ E_2 &= \sin p_i T_N \cos q_{i-1} T_N, \\ E_3 &= \cos p_{i-1}\tau \cos q_{i-1}\tau, \\ E_4 &= \sin p_{i-1}\tau sinq_{i-1}\tau, \\ E_5 &= \cos p_i\tau \cos q_i\tau, \\ E_6 &= \sin p_i\tau \sin q_i\tau, \\ E_7 &= \sin p_{i-1} T_N \cos q_{i-2} T_N, \\ E_8 &= \cos p_{i+1} T_N \sin q_i T_N, \\ E_9 &= \cos n_{i-1}\tau, \\ E_{10} &= \cos n_i\tau \end{aligned} \quad (4)$$

and

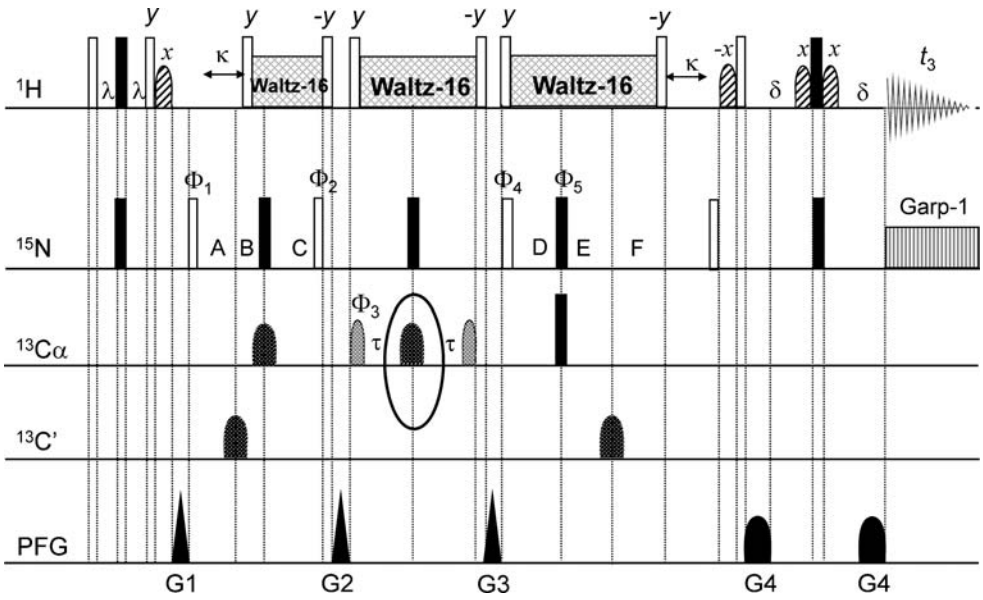

Fig. 1 Pulse sequence for the HNN-ST experiment. Narrow (hollow) and wide (filled black) rectangular bars represent non-selective 90° and 180° pulse, respectively. Narrow lobe (light) and wide lobe (dark) on carbon channel indicate selective 90° and 180° pulse, respectively. Unless indicated otherwise, the pulses are applied with phase x. The ^{1}H and ^{15}N carrier frequencies are set at 4.71 ppm (water) and 119.0 ppm, respectively. The ^{13}C carrier frequency is set at 56.0 ppm, except for the encircled pulse on carbon channel, where it is set at 64.0 ppm. Proton decoupling using the Waltz-16 decoupling sequence (Shaka et al. 1983a, b) with field strength of 6.3 kHz is applied during most of the t_1 and t_2 evolution periods, and ^{15}N decoupling using the Garp-1 sequence (Shaka et al. 1985) with field strength 0.9 kHz is applied during acquisition. The strength of the $^{13}C^{\alpha}$ pulses (standard Gaussian cascade Q3 pulse) (Emsley and Bodenhausen 1990) is adjusted so that they cause minimal excitation of carbonyl carbons. The band-selective 180° pulse in the experiment – responsible for tunability and versatility of HNN – is encircled for emphasis. The 180° ^{13}CO shaped pulse (width 0.6 ms) had a standard Gaussian cascade Q3 pulse profile with minimum excitation of $^{13}C^{\alpha}$. The delays are set to $\lambda = 2.7$ ms, $\kappa = 5.4$ ms and $\delta = 2.7$ ms. τ must be optimized and is around 12–16 ms. The values for the individual periods containing t_1 are: A = $t_1/2$, B = T_N, and C = $T_N - t_1/2$. The values for the individual period containing t_2 are: D = $T_N - t_2/2$, $E = T_N$, and $F = t_2/2$. Phase cycling for the experiment is $\Phi_1 = 2(x)$, $2(-x)$; $\Phi_2 = \Phi_3 = x$, $-x$; $\Phi_4 = 4(x)$, $4(-x)$; $\Phi_5 = x$ and receiver = $2(x)$, $4(-x)$, $2(x)$. Frequency discrimination in t_1 and t_2 has been achieved using States-TPPI phase cycling (Marion et al. 1989) of Φ_1 and Φ_4, respectively, along with the receiver phase. The gradient (sine-bell shaped; 1 ms) levels are as follows: G_1 = 30%, G_2 = 30%, G_3 = 30% and G_4 = 80% of the maximum strength 53 G/cm in the z-direction

$$
\begin{aligned}
&p_i = 2\pi^1 J\left(\mathrm{C}_i^{\alpha} - \mathrm{N}_i\right); \quad q_i = 2\pi^2 J\left(\mathrm{C}_i^{\alpha} - \mathrm{N}_{i+1}\right);\\
&n_i = 2\pi^1 J\left(\mathrm{C}_i^{\alpha} - \mathrm{C}_i^{\beta}\right),
\end{aligned} \tag{5}
$$

$$
\begin{aligned}
K_{i1}^{d} &= \exp\left(-4T_N R_{2,i}^{N} - 2\tau R_{2,i-1}^{\alpha}\right),\\
K_{i2}^{d} &= \exp\left(-4T_N R_{2,i}^{N} - 2\tau R_{2,i}^{\alpha}\right),\\
K_{i-1}^{c} &= \exp\left(-2T_N\left(R_{2,i}^{N} + R_{2,i-1}^{N}\right) - 2\tau R_{2,i-1}^{\alpha}\right),\\
K_{i+1}^{c} &= \exp\left(-2T_N\left(R_{2,i}^{N} + R_{2,i+1}^{N}\right) - 2\tau R_{2,i}^{\alpha}\right).
\end{aligned} \tag{6}
$$

^{1}J and ^{2}J's represent, respectively, the one-bond and two-bond N–C^{α} coupling constants, R_2's correspond to the various transverse relaxation rates.

A detailed analysis of the above equations reveals that the terms E_1–E_8 have a positive value for optimum choice of transfer periods (12–14 ms), whereas, E_9 and E_{10} remain negative (~ -1.0). This results in a positive diagonal peak, (I_i^d, Eq. 2), and two negative sequential peaks, (I_{i-1}^c and I_{i+1}^c; Eq. 3). However, in the case of glycines, C^{α}–C^{β} coupling evolution does not occur, and consequently, either E_9 or E_{10} term will be absent, depending on whether glycine is present at the $(i-1)$ or i position. For example, for a glycine at i, E_{10} term would be absent and if $(i-1)$ is a non-glycine, then Eqs. 2 and 3 get modified as below:

$$
I_i^d = -\left(E_1^2 E_3 E_9 K_{i1}^d + E_2^2 E_5 K_{i2}^d\right) \tag{7}
$$

$$
I_{i-1}^c = E_1 E_4 E_7 E_9 K_{i-1}^c; \quad I_{i+1}^c = E_2 E_6 E_8 K_{i+1}^c \tag{8}
$$

Now, the terms $E_1^2 E_3 E_9 K_{i1}^d$ and $E_2^2 E_5 K_{i2}^d$ in Eq. 7 would be negative and positive, respectively, and of these the second term is larger than the first term. As a result the overall value of I_i^d becomes negative. Similarly, I_{i-1}^c and I_{i+1}^c would be negative and positive, respectively, (Eq. 8). Glycines, thus, generate a special pattern for $i-1$, i, and $i+1$ residues (Bhavesh et al. 2001) – negative i, $i-1$ and positive $i+1$th peaks as against positive ith and negative $i-1$, $i+1$th peaks for non-glycine residues – and serve as start/check points for the sequential walk in the HNN spectrum. These peak patterns would be different when glycine is present in

($i - 1$) position and a detailed analyses for all such patterns has already been presented (Bhavesh et al. 2001).

We realize from above that magnetization evolution during the 2τ period (C^{α} evolution) plays a crucial role in determining the peak patterns in the HNN spectrum. It can be recognized easily that by tampering with the C^{α} evolution, especially with the C^{α}–C^{β} coupling evolution, during this period, it should be possible to manipulate the peak patterns for specific residues. In this context the 180° pulse (encircled in Fig. 1), which serves the purpose of (i) refocusing C^{α} chemical shifts and (ii) keeping active evolutions under C^{α}–C^{β} coupling and C^{α}–N coupling, plays a crucial role. Three different possibilities can be conceived and this is dictated by the ranges and distinctiveness of the C^{α} and C^{β} chemical shifts of the different residue types (see Fig. 2):

(i) The C^{α} chemical shifts of glycines are very distinct (40–45 ppm) and the 180° pulse can be made very selective to refocus only these residues. In such a situation, since the non-glycine C^{α}s do not see the 180° pulse, the corresponding nitrogens will be decoupled and in the absence of C^{α}–N coupling evolution, there will be no transfer of magnetization to the neighboring residues. However, this transfer can be recovered by making the synchronous 180° pulse on the nitrogen channel (see Fig. 1) also selective to cover only the glycine nitrogen chemical shifts. But in the end there is really no significant advantage in the 3D spectrum with regard to the peak patterns, as C^{α}–C^{β} coupling evolution remains unperturbed.

(ii) The C^{β} chemical shift of alanines is very distinct (18–20 ppm). The 180° pulse can be made band selective not to invert the C^{β} of alanines. This will eliminate C^{α}–C^{β} coupling evolution for these residues and make them look like glycines in the 3D spectrum. This was recently described as HNN-A (Chatterjee et al. 2006).

(iii) The C^{β} chemical shift of serines and threonines are most downfield shifted (60–79 ppm) compared to all other amino acid residues (18–43 ppm) (Fig. 2). Then a band-selective 180° pulse applied to selectively refocus all the non-glycine C^{α} carbons (note that any attempt to include C^{α} carbons of glycines results in inversion of several C^{β} carbons as well) in the range of 49–79 ppm, would avoid C^{α}–C^{β} coupling evolution for all the residues except for serines and threonines – for which the C^{β} (60–79 ppm) also gets refocused during the same time and C^{α}–C^{β} coupling evolves in a normal manner. This modification has, however, another consequence. Since the 180° pulse excludes C^{α} of glycines as well, there will also be no evolution under C^{α}–N coupling for glycines. As a result there will be no transfers of magnetization from the glycines to the neighboring residues. Consequently, the peak patterns in the different planes of the 3D spectrum for triplet of residues containing glycines will get modified compared to those in the normal HNN spectrum. We have calculated all these patterns by setting the appropriate coupling constants to zero when evolutions under them have to be ignored. All the expected peak patterns in this experiment are presented in the next section. We term this experiment as HNN-ST.

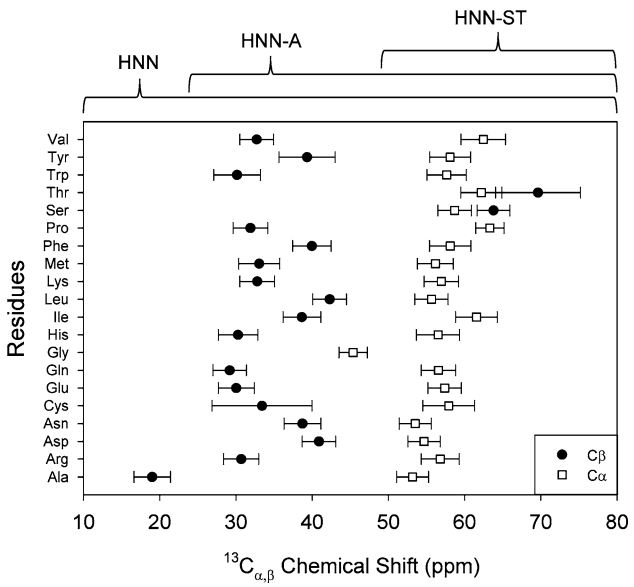

Fig. 2 Comparison of refocusing bandwidths in $^{13}C^{\alpha,\beta}$ region for HNN, HNN-A and HNN-ST spectra. $^{13}C^{\alpha}$ and $^{13}C^{\beta}$ average chemical shifts for 20 common amino acid residues were plotted against the residue types. These average chemical shifts were taken from the statistical table containing values calculated from the full BMRB database (http://www.bmrb.wisc.edu/ref_info/statful.htm#1). This includes paramagnetic proteins, proteins with aromatic prosthetic groups, and entries where chemical shifts are reported relative to uncommon chemical shift references. Standard deviation in these values is plotted as error bars

The HNN-ST experiment has one small advantage compared to HNN and that is in the sensitivities of the diagonal and the sequential peaks. This arises from the fact that the terms E9 and E10 (in Eqs. 2 and 3) will be uniformly unity for all non-serine/threonine residues. For the typical 11–12 ms choice of τ value and a C^{α}–C^{β} coupling constant of 35 Hz, this yields a roughly 10% gain in sensitivity.

Distinctive peak patterns in HNN-ST

For the purpose of sequential resonance assignment in labeled proteins, it would be useful to have a catalogue of

specific patterns in the spectra. As described for HNN (Bhavesh et al. 2001) and HNN-A (Chatterjee et al. 2006), triplets of residues may be considered here as well for various patterns of positive and negative signs for the diagonal and sequential peaks. It will be evident from the previous discussion that in the HNN-ST experiment, the sign of the serine and threonine diagonal peak will always remain opposite to that of any other residue; the actual sign would, however, depend upon the phasing of the spectrum. We have chosen the diagonal of serine and threonine to have a negative sign; this would be opposite to what one would simply obtain from Eq. 2. Accordingly the sequential peaks (Eq. 3) would also change sign. By doing so, the peak patterns obtained for serines and threonines exactly match the ones obtained for glycines in the HNN spectrum (Bhavesh et al. 2001), with glycines being replaced by serines/threonines. For example, the pattern for XSZ or XTZ in HNN-ST (X and Z are not serine or threonine) would be similar to that for XGZ (X and Z are not glycine) in the normal HNN. More importantly, the patterns for most other triplets excepting those containing glycines and serine/threonines would be very similar to those in normal HNN. This is important to avoid confusions when one is using variants of HNN for the sequential walk. Glycines in HNN-ST, however, would behave slightly differently due to decoupling of C^{α}–N couplings during the 2τ period. The various patterns thus obtained are explicitly described in Fig. 3.

We have categorized different triplet of residues in nine following ways: (I) ZXZ′; (II) PXZ, ZXP, PXP; (III) PXB, PBX, PBB′, BXP, B′BP, XBP, PBP; (IV) XBZ, BXZ, ZXB, B″BZ, ZBB′, B″ZB′, B″BB′; (V) PXG, PGX, PGG′, GXP, G′GP, XGP, PGP; (VI) GBP, PBG, PGB, BGP; (VII) GBX, BXG, XGB, XBG, GXB, BGX; (VIII) G′GB, G′BG, BGG′, B′BG, B′GB, GBB′; and (IX) XGZ, GXZ, ZXG, G″GZ, ZGG′, G″XG′, G″GG′, where X, Z and Z′ are any residue other than proline, glycine, serine/threonine. G, G′ and G″ are glycines, P is proline, and B, B′ and B″ stand for serine/threonine in the sequence. Category I is a general one not containing any glycine, proline, serine/threonine and has been included to be able to distinguish the special patterns from the general pattern, category II has prolines but no glycines and serines/threonines, category III has combinations of prolines and serines/threonines, category IV has serines/threonines but no glycines and prolines, category V has combinations of prolines and glycines, category VI has combinations of glycines, serines/threonines and prolines, category VII has combinations of glycines and serines/threonines but no prolines, category VIII has combination of two glycines and one/serine/threonine and vice versa, and category IX has only glycines. Diagonal peaks are shown by squares and sequential peaks by circles; filled circles/squares are for positive peaks and open circles/squares are for negative peaks. These patterns enable unambiguous discrimination between the triplets having glycines, triplets having serines/threonines and triplets having X as the central residue. However, careful examination reveals that for the triplets where glycine or proline is at the $i-1$ position the patterns will be similar and this can lead to some ambiguities (see for example,

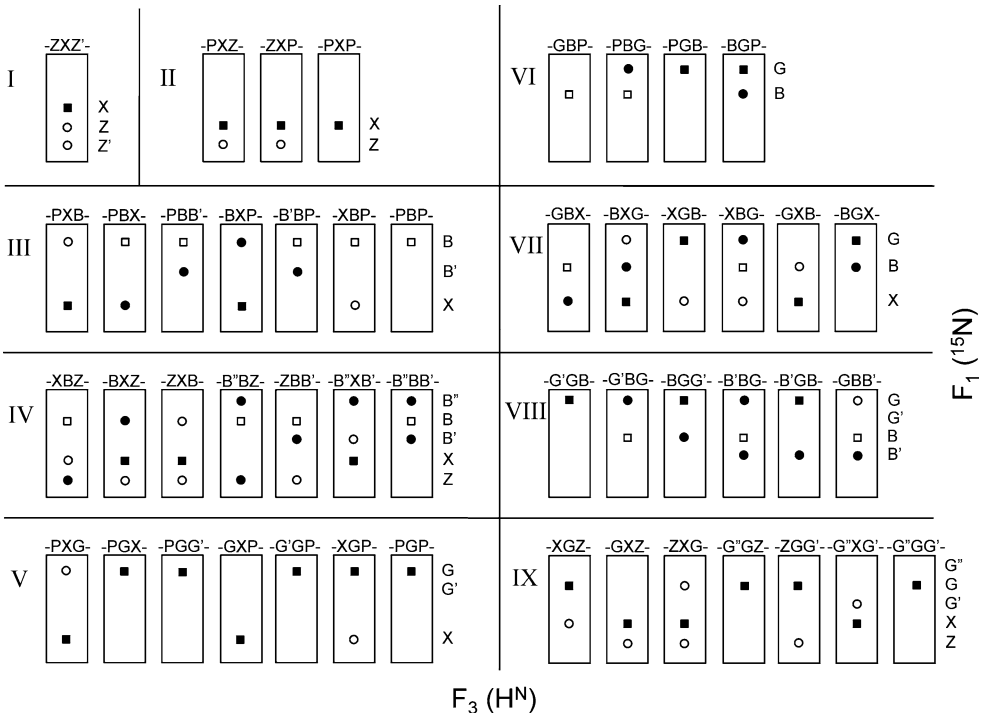

Fig. 3 Schematic patterns in the $F_1(^{15}N)$–$F_3(H^N)$ planes at the $F_2(^{15}N)$ chemical shift of the central residues in the triplets mentioned on top of each panel in HNN-ST spectra for various special triplet sequences of categories I–IX (see text). X, Z and Z′ are any residue other than proline, glycine, serine/threonine. G, G′ and G″ are glycines, P is proline, and B, B′ and B″ stand for serine/threonines in the sequence. Diagonal peaks are shown by squares and sequential peaks by circles where filled circles/squares are for positive peaks and open circles/squares are for negative peaks. In all the cases the peaks are aligned at the $F_3(H^N)$ chemical shift of the central residue

PXZ vs. GXZ; PBX vs. GBX; among the triplets PGX, PGG, GXP, GGP, PGP, GGZ, GGG and GGB etc.). In these situations the ambiguities can be readily resolved by comparing with the corresponding patterns in the HNN or HNN-A spectrum.

We have tested the HNN-ST experiment with two proteins under different conditions: M-crystallin protein (apo form; folded; 85 residues) and urea-denatured dsmt3 (denatured protein; 88 residues). For both these systems assignments have already been published (Kumar et al. 2007; Barnwal et al. 2006) and thus they served as excellent test cases. In either case almost all the expected correlations were observed in the HNN-ST spectrum. Figure 4 shows a comparison of the HNN and HNN-ST patterns for all the eight serine and threonine residues in the case of urea denatured dsmt3. All of these belong to XBZ stretches; assignments used here have been reported in (Kumar et al. 2007). In the first strip (S2 diagonal, HNN, Fig. 4) peaks corresponding to M1 and D3 residues have an overlap in $F_1(^{15}N)$ dimension, but these are resolved in HNN-ST experiment due to different signs of those sequential peaks. Similar is the case in the third strip (S49 diagonal, Fig. 4), where L48 and M50 overlap in HNN but are resolved in HNN-ST; position corresponding to L48 is encircled in dash to show that the peak is not present at this contour threshold. In the last strip (T86 diagonal, Fig. 4), G87 peak is present in HNN-ST experiment in a normal manner and its pattern is described by triplet XBG which is depicted in panel VII of Fig. 3.

Figure 5 shows a sequential walk illustration through HNN-ST in the case of a folded protein, namely, M-crystallin; assignments used here have been reported in (Barnwal et al. 2006). It also demonstrates the value of the distinctive patterns as check points during the sequential walks. The G64 plane (Fig. 5) has only one peak since the residue at position 63 is a proline which does not produce any peak and peak corresponding to $i + 1$th position will be absent (dashed circle), this belongs to triplet PGX depicted in panel V of Fig. 3. Note here that the diagonal of glycine is positive. The E65 plane has two peaks, one diagonal and the other, $i + 1$ sequential; this plane belongs to triplet GXZ and is depicted in panel IX of Fig. 3. The pattern for Y66 belongs to triplet ZXB (panel IV of Fig. 3) and is the same as that for ZXG in HNN (data not shown). This is consistent with the description given above. Further the patterns for S67 and S68 planes (triplets ZBB′ and B″BZ, panel IV, Fig. 3) are as must be expected for the HNN-ST.

It is thus clear that the HNN-ST experiment together with HNN and HNN-A provides a substantial boost to the sequential assignment process in labeled proteins. It will be particularly of greater value if the protein sequence has none or few far apart glycines and alanines along the amino acid sequence of the polypeptide chain. We envisage that these would be very helpful for the backbone assignment of

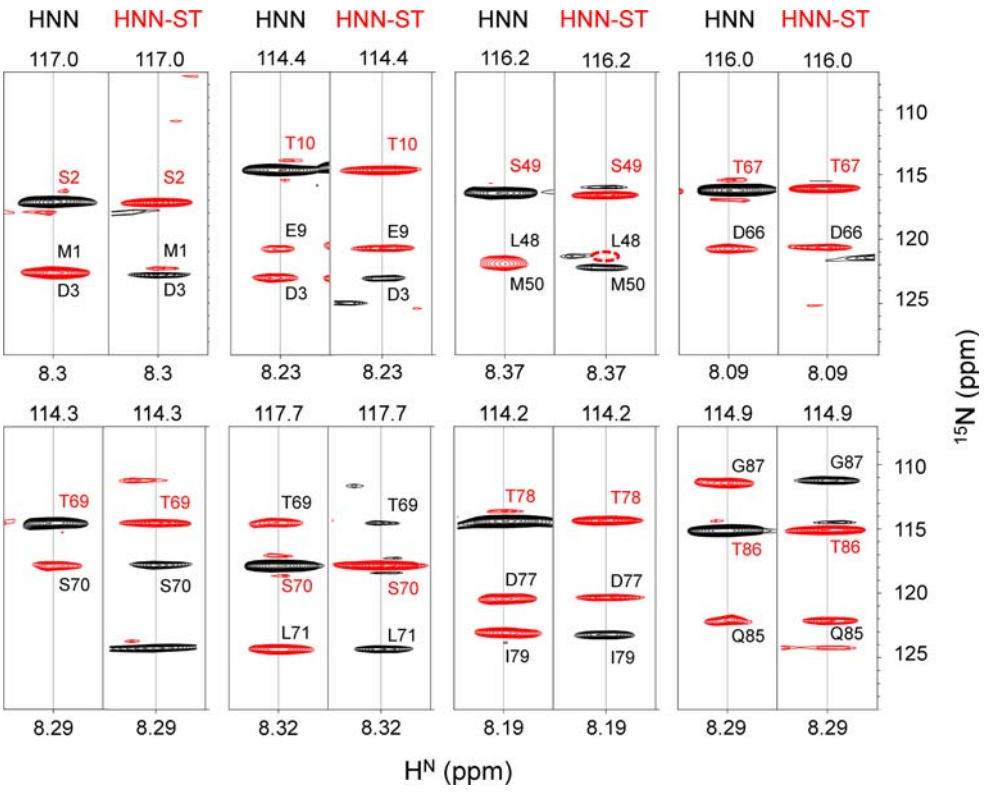

Fig. 4 Comparison of $F_1(^{15}N)$–$F_3(H^N)$ strips of the HNN and the HNN-ST spectra for all the eight serine and threonine residues in the case of urea-denatured dsmt3 protein. The $F_2(^{15}N)$ values, which help to identify diagonal peaks, are shown at the top for each strip. The black and red contours indicate positive and negative peaks, respectively. The residues corresponding to diagonal peaks in each strip are marked in red. The distinguishing behavior for all the serine (Ser) and threonine (Thr) residues is evident from the negative diagonal peaks. These residues also serve as start points for the sequential walk, as $i - 1$th peak is negative and $i + 1$th peak is positive in HNN-ST spectra. Position for L48 peak in the HNN-ST spectra is encircled by dashed line to show that the peak is not present at this contour threshold

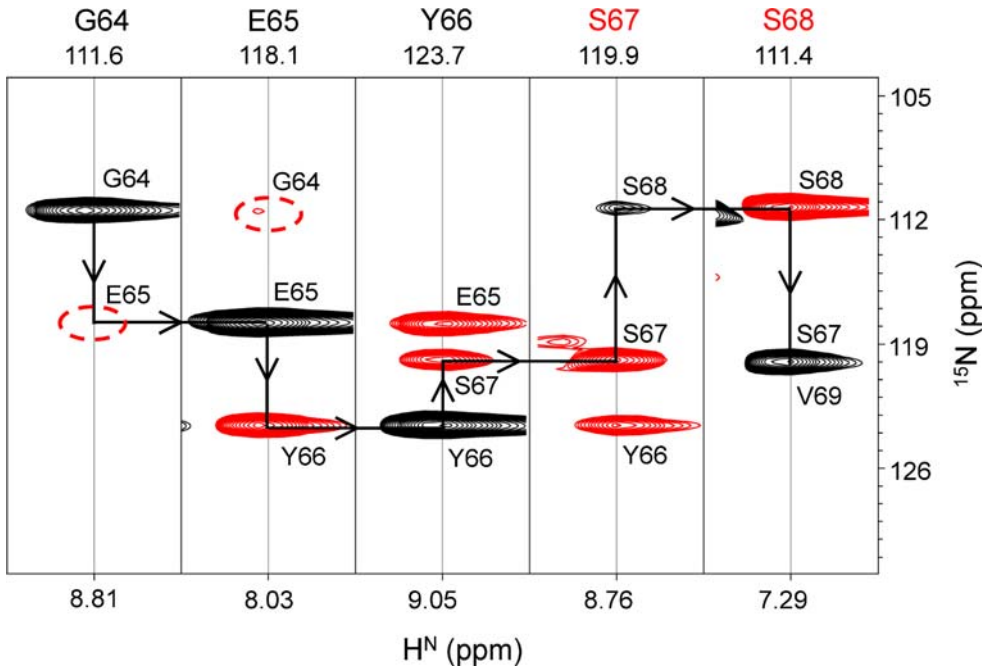

Fig. 5 Illustrative sequential walk through $F_1(^{15}N)$–$F_3(H^N)$ planes of HNN-ST spectra for M-crystallin protein (apo form; folded) in 50 mM Tris buffer containing 150 mM KCl at pH 7.5. The $F_2(^{15}N)$ values, which help to identify diagonal peaks, and the residues corresponding to diagonal peaks are shown at the top for each strip. The black and red contours indicate positive and negative peaks, respectively. The position for i + 1th peak (E65) in the G64 diagonal-plane and i − 1th peak (G64) in the E65 diagonal-plane is encircled to emphasize the absence of those peaks due to selective refocusing of all non-glycine C^{α} carbons (see text). S67 and S68 labels at the top are in red to emphasize the distinctive feature of these diagonal peaks as is evident from their negative sign

large proteins where large number of anchor points would be required. However, one concern in this context would be the inherently low sensitivity of these experiments compared to the more common triple resonance experiments such as HNCA, HNCO, etc. Nonetheless, with the availability of high fields and high sensitivity probes at the present times, and by incorporation of the TROSY option (Pervushin et al. 1997) in the pulse sequences along with perdeuteration of the proteins to reduce relaxation losses the sensitivity problems can be circumvented. While we do have the appropriately modified pulse sequences, we have to wait for the availability of a suitable, well-behaved large protein to demonstrate their application. Further, the fact that all the three experiments have been found to be working extremely well for both folded and unfolded proteins [this work and (Bhavesh et al. 2001; Chatterjee et al. 2006)] establishes the versatility of the HNN suite of experiments.

The ideas described here can be readily extended to the HN(C)N pulse sequence (Panchal et al. 2001); it can also be tuned to generate an HN(C)N-ST experiment in a similar manner.

Acknowledgements We thank Government of India for providing financial support to the National Facility for High Field NMR at Tata Institute of Fundamental Research, India. We thank Mr. Ravi Pratap Barnwal for the sample of M-crystallin. We acknowledge Dr. Shilpy Sharma for the active discussions during the manuscript preparation. Jeetender Chugh is the recipient of TIFR Alumni Association fellowship for career development though the years 2002–2005.

References

Barnwal RP, Jobby MK, Sharma Y, Chary KV (2006) NMR assignment of M-crystallin: a novel Ca^{2+} binding protein of the $\beta\gamma$-crystallin superfamily from *Methanosarcina acetivorans*. J Biomol NMR 36(Suppl 1):32

Bhavesh NS, Panchal SC, Hosur RV (2001) An efficient high-throughput resonance assignment procedure for structural genomics and protein folding research by NMR. Biochemistry 40:14727–14735

Bracken C, Palmer AG III, Cavanagh J (1997) (H)N(COCA)NH and HN(COCA)NH experiments for 1H–15N backbone assignments in 13C/15N-labeled proteins. J Biomol NMR 9:94–100

Chatterjee A, Bhavesh NS, Panchal SC, Hosur RV (2002) A novel protocol based on HN(C)N for rapid resonance assignment in ((15)N, (13)C) labeled proteins: implications to structural genomics. Biochem Biophys Res Commun 293:427–432

Chatterjee A, Kumar A, Hosur RV (2006) Alanine check points in HNN and HN(C)N spectra. J Magn Reson 181:21–28

Emsley L, Bodenhausen G (1990) Gaussian pulse cascades: new analytical functions for rectangular selective inversion and in-phase excitation in NMR. Chem Phys Lett 165:469–476

Fiorito F, Hiller S, Wider G, Wuthrich K (2006) Automated resonance assignment of proteins: 6D APSY-NMR. J Biomol NMR 35:27–37

Grzesiek S, Anglister J, Ren H, Bax A (1993) Carbon-13 line narrowing by deuterium decoupling in deuterium/carbon-13/nitrogen-15

enriched proteins. Application to triple resonance 4D J connectivity of sequential amides. J Am Chem Soc 115:4369–4370

Hiller S, Wasmer C, Wider G, Wuthrich K (2007) Sequence-specific resonance assignment of soluble nonglobular proteins by 7D APSY-NMR spectroscopy. J Am Chem Soc 129:10823–10828

Kumar D, Kumar A, Misra JR, Chugh J, Sharma S, Hosur RV (2007) 1H, 15N, 13C resonance assignment of folded and 8 M urea denatured state of SUMO from *Drosophila melanogaster*. Biomol NMR Assignment (Online first available at doi: 10.1007/s12104-007-9072-6)

Marion D, Ikura M, Tschudin R, Bax A (1989) Rapid recording of 2D NMR spectra without phase cycling. Application to the study of hydrogen exchange in proteins. J Magn Reson 85:393–399

Matsuo H, Kupce E, Li H, Wagner G (1996) Use of selective C alpha pulses for improvement of HN(CA)CO-D and HN(COCA)NH-D experiments. J Magn Reson B 111:194–198

Panchal SC, Bhavesh NS, Hosur RV (2001) Improved 3D triple resonance experiments, HNN and HN(C)N, for HN and 15N sequential correlations in (13C, 15N) labeled proteins: application to unfolded proteins. J Biomol NMR 20:135–147

Permi P, Annila A (2003) Coherence transfer in proteins. Prog Nucl Magn Reson Spectrosc 44:97–137

Pervushin K, Riek R, Wider G, Wuthrich K (1997) Attenuated T2 relaxation by mutual cancellation of dipole–dipole coupling and chemical shift anisotropy indicates an avenue to NMR structures of very large biological macromolecules in solution. Proc Natl Acad Sci USA 94:12366–12371

Piotto M, Saudek V, Sklenar V (1992) Gradient-tailored excitation for single-quantum NMR spectroscopy of aqueous solutions. J Biomol NMR 2:661–665

Shaka AJ, Keeler J, Frankiel T, Freeman R (1983a) An improved sequence for broadband decoupling: WALTZ-16. J Magn Reson 52:335–338

Shaka AJ, Keeler J, Freeman R (1983b) Evaluation of a new broadband decoupling sequence: WALTZ-16. J Magn Reson 53: 313–340

Shaka AJ, Barker PB, Freeman R (1985) Computer-optimized decoupling scheme for wideband applications and low-level operation. J Magn Reson 64:547–552

Weisemann R, Ruterjans H, Bermel W (1993) 3D triple-resonance NMR techniques for the sequential assignment of NH and 15N resonances in 15N- and 13C-labelled proteins. J Biomol NMR 3: 113–120